

Study of Mechanical and Wear Behaviour of Hyper-Eutectic Al-Si Automotive Alloy Through Fe, Ni and Cr Addition

Mohammad Salim Kaiser^{a,*}, Sakib Hasan Sabbir^b, Mohammad Syfullah Kabir^b,

Mashiur Rahman Soummo^b, Maglub Al Nur^b

^aDirectorate of Advisory, Extension and Research Services, Bangladesh University of Engineering and Technology, Dhaka, Bangladesh

^bDepartment of Mechanical Engineering, Bangladesh University of Engineering and Technology, Dhaka, Bangladesh

Received: December 15, 2017; Revised: February 20, 2018; Accepted: April 20, 2018

Effect of Fe, Ni and Cr addition on the wear behavior of hyper-eutectic Al-Si automotive alloy has been studied. Dry sliding wear tests have been conducted using pin-on-disc wear testing machine under normal loads of 20N and constant sliding speed of 0.64 ms⁻¹. Influence of Fe addition to the base alloy increases the wear rate due to the formation of needle beta intermetallics. Ni addition to the alloy does not impede formation of needle-like intermetallic compounds and has no positive effect on the modification of microstructure. Introducing of Cr to the iron-rich alloy changes the beta intermetallics into the modified alpha phases and therefore reduced the detrimental effect of iron. As a result it recovers the strength and wear properties of the experimental alloy. Wear test surfaces were examined by SEM and have shown that Cr added alloy improves wear resistance through mild and smooth abrasive grooves filled with oxides.

Keywords: Hyper-eutectic Al-Si alloy, wear, worn surfaces, SEM.

1. Introduction

Hypereutectic aluminium-silicon alloys are used in applications that require high resistance to wear, corrosion, good mechanical properties, low thermal expansion and reduced density^{1,2}. Their properties are of greatest attention to the automobile industry for the fabrication of fuel-efficient vehicles using light weight components produced from these alloys such as connecting rods, pistons, cylinder liners and engine blocks³⁻⁵. The good mechanical properties and high resistance to wear are basically recognized to the presence of hard primary silicon particles spread in the metal matrix^{6,7}. The wear resistance can, however, also be affected by Si in the eutectic matrix. Hyper-eutectic Al-Si alloys can be considered as in situ metal matrix composites, where the primary silicon acts as the reinforcing phase^{8,9}. This class of materials acquires its high strength and stiffness from the reinforcing phase and the damage tolerance and toughness is provided by the metal matrix¹⁰. However, the high latent heat and consequent long solidification time of hypereutectic Al-Si alloys results in excessive growth of primary silicon particles as well as unfavourable shrinkage behavior which adversely affects the use of these alloys¹¹.

The quality of cast-off Al-Si alloys is considered to be a most important issue in selecting an alloy casting for a particular purpose. Cu or Mg and certain amount of Fe, Mn and more, that are present either accidentally or they are added purposely to offer special material properties of Al-Si alloys. These elements partly go into solid solution in the matrix and partly form intermetallic particles during solidification. The morphology of intermetallic and the size, volume depends on the solidification conditions and heat treatment of the alloys^{12,13}.

The existence of higher amount of iron in Al-Si alloys is unwanted, because it forms brittle and hard intermetallic phases. Be, Cr, Mn, Co, Sr, Ca and RE change the morphology of platelet iron intermetallic compound to harmless shapes and hence improve the mechanical properties. Nickel also acts as an iron corrector of the alloys^{14,15}. Wear resistance is one of the most important properties of these alloys. The wear response of the alloys significantly depends on their hardness, tensile strength, brittleness, microstructure etc. Research and development on various types of Al-Si-Fe alloy have been actively carried out to improve the tribological properties of such alloys¹⁶⁻¹⁹. The aim of this work is thus to study the effect of increasing Fe additions on the wear behaviour of the hyper-eutectic Al-Si automotive alloy and the role of Ni and Cr on the Fe added alloys.

*e-mail: mkskaiser@iat.buet.ac.bd

2. Experimental details

A laboratory type ceramic fiber resistance heating furnace under the suitable flux cover (degasser, borax etc.) was used for melting. The chamber size of the furnace was 450 x 450 x 450mm with a perfect for maximum and continuous working temperature of 930°C. First the aluminium engine block was melted in a #8 10 kg clay-graphite crucible which was used as the master alloy. Four heats were taken for developing Al-Si base alloy, Al-Si containing Fe, Ni, and Cr. The final temperature of the melt was always maintained at 750±15°C. Casting was done in cast iron metal moulds preheated to 200°C. Mould sizes were 16 x 150 x 300 in millimeter. The alloys were analysed by spectrochemical method. The chemical composition of the alloys is given in Table 1. The cast alloys were homogenized in a Muffle furnace at 400°C for 18 hours and air cooled to relieve internal stresses. The homogenized samples was solutionized at 530°C for 2 hours followed by salt ice water quenching to get a super saturated single phase region. The sample of 12 mm length and 5 mm diameter were machined from the experimental alloys for wear study by following ASTM Standard G99-05. For the study the samples were aged at 175°C for 240 minutes to attend the peak aged condition^{20,21}. Density of the alloys were calculated from the chemical composition of the alloys. Hardness of aged alloys was measured in Vickers hardness testing machine at 2 kg load and an average of ten concordant readings was taken as the representative hardness of a sample. Tensile testing was carried out at room temperature in an Instron testing machine using cross head speed to maintain the strain rate of 10⁻³/s. The samples used were according to ASTM specification. For impact test, standard sized of 10 x 10 x 55 mm have a V-shaped notch, 2 mm deep with 45° angle specimens were used. Testing was performed in accordance with ASTM E23. Tensile and Impact toughness were determined five test pieces at each test. Mild steel discs were used as the counter-body material. The hardness of the mild steel discs was around RC 50. One of the surfaces of the disc was grinded by surface grinding machine and cleaned with cotton. The frictional and wear behaviors of the aluminium alloys were investigated in a pin-on disc type wear apparatus by following ASTM Standard G99-05²². During the wear tests, the end surface of the pin samples were pressed against horizontal rotating cast iron disc. Load of 20N was used throughout the test, which yielded nominal contact pressures of 1.0MPa. The

tests were conducted at the sliding speed of 0.64 ms⁻¹ with varying sliding distances ranging from 200m-4600m. All the tests were carried out in ambient air (humidity 70%) under dry sliding condition (without lubrication). After completion of wear tests, samples were cleaned with acetone. At least three tests were done for each type of material. The sliding distances were calculated by knowing the track diameter and speed of rotation of the disc. Wear rates were calculated from average values of weight-loss measurements. Wear rate (WR) was estimated by measuring the mass loss (ΔW) after each test. It is calculated as the ratio of ΔW to sliding distance (SD) and applied load L ^{16,22}:

$$WR = \frac{\Delta W}{SD \times L} \quad (1)$$

Microstructural observation of the worn specimens were done carefully by using USB digital microscope and some selected photomicrographs were taken. The SEM investigation was conducted by using a JEOL scanning electron microscope.

3. Results and Discussion

3.1. Physical and mechanical properties

Fig. 1 shows the density of the experimental alloys. Base Alloy 1 shows the lower density, Fe added Alloy 2 shows higher density because it contents about 6% Fe, similarly Fe and Ni added Alloy 3 contents about 0.6% Ni and Fe, Ni and Cr added Alloy 4 contents about 1.3% Cr. Fig. 2 shows the variation of the microhardness of the alloys at peak aged condition. Except the base Alloy 1 all the alloys attain the higher hardness. It is due to higher amount of Fe in the alloys led to formation of variety of Fe-rich intermetallic phases in aluminium alloys as Al₃Fe, α -Al₈Fe₂Si, β -Al₃FeSi, δ -Al₄FeSi₂ and γ -Al₃FeSi, specially hard β -Al₃FeSi phase²³. Some improvement is observed in Ni added Alloy 3 due to precipitation of Ni intermetallic into the aluminium matrix. The Cr added Alloy 4 losses small amount of the hardness because Cr modify the morphology and type of Fe rich intermetallic phases in cast aluminum alloys. Fig. 3 shows the ultimate tensile strength of the experimental alloys at peak aged condition. The tensile strength of the Fe added Alloy 2 decreases due to formation of iron intermetallic compounds with aluminum and several other elements present in the alloy exhibiting a variety of morphologies.

Table 1. Chemical composition of the experimental alloys (wt%)

Alloy	Si	Fe	Ni	Cr	Cu	Mg	Zn	Mn	Ti	Al
1	19.209	0.795	0.089	0.040	2.826	0.245	1.117	0.214	0.099	Bal
2	17.947	5.910	0.091	0.086	2.881	0.186	1.139	0.183	0.071	Bal
3	18.913	6.256	0.567	0.057	2.889	0.193	1.124	0.178	0.090	Bal
4	19.363	5.501	0.621	1.267	3.112	0.232	1.085	0.217	0.076	Bal

Such morphologies of the iron-bearing phase is known to play a deciding role in the alloys strength²³. Ni added Alloy 3 continue the nature with some improvement. It is due to formation of Ni intermetallics in to the Al matrix. Cr added Alloy 4 recovers the strength of the alloy. In case of elongation and impact energy similar results are shown in Fig. 4 and Fig. 5 respectively. Presence of higher amount of Fe in the hyper-eutectic Al-Si automotive alloy remarkable decreases the properties of the alloys. These Fe bearing intermetallic compounds are very hard and brittle. It ensue as stress raisers and points of weakness that reduce the strength and ductility of the alloy. They exist as separate particles with a highly faceted nature in the alloy matrix. Therefore, it has comparatively low bond strength with the matrix causes the minimum impact strength^{24,25}. Nickel addition creates different intermetallics which slightly increase the alloy's strength, it also take steps as an iron corrector, if not nickel reduces ductility¹⁵. The addition of Cr change in their effectiveness to modify the harmful β phase. Cr addition has stimulated the conversion of a harder phase of β -Al₃FeSi to α -Al(Fe, Cr)Si. For the ductility, α -Al(Fe, Cr)Si has a more positive effect attributed to its more rounded appearance comparing with needle-like β -Al₃FeSi²⁶.

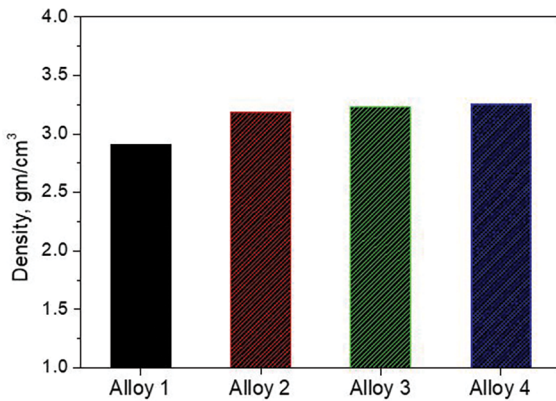


Figure 1. Variation of density of the experimental alloys.

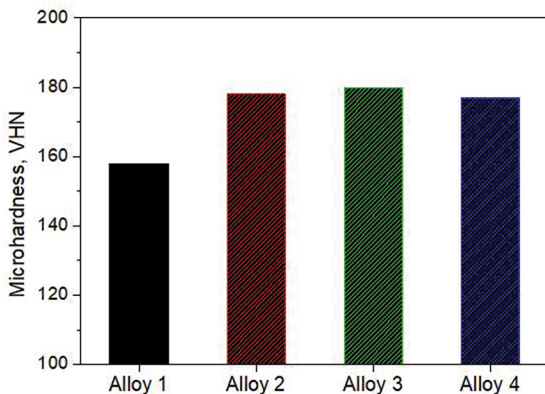


Figure 2. Variation of microhardness of the experimental alloys.

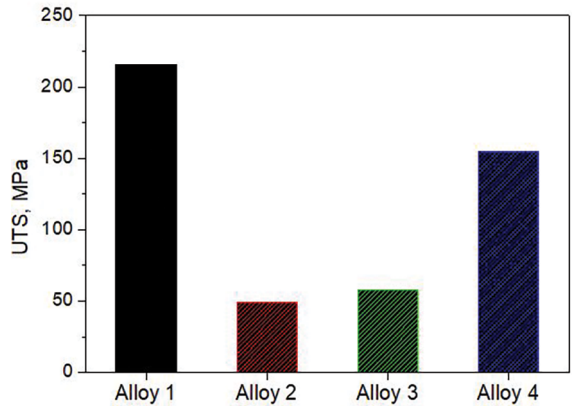


Figure 3. Variation of ultimate tensile strength of the experimental alloys.

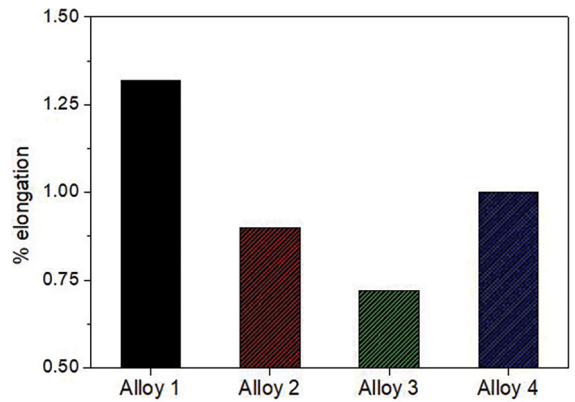


Figure 4. Variation of % elongation of the experimental alloys.

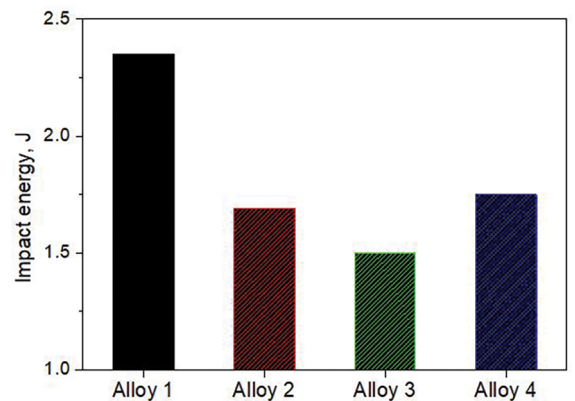


Figure 5. Variation of impact energy of the experimental alloys.

3.2. Wear behaviour

The weight loss, as a function of sliding distance for all the alloys at constant pressure of 20 N and velocity of 0.64 ms⁻¹ is shown in figure 6. The weight loss of the alloys increases with sliding distance but the Fe and Ni added Alloy 3 increases more rapidly compared to the other alloys. When the sliding distance increases the duration of contact between the surfaces also increased, therefore more weight loss are observed.

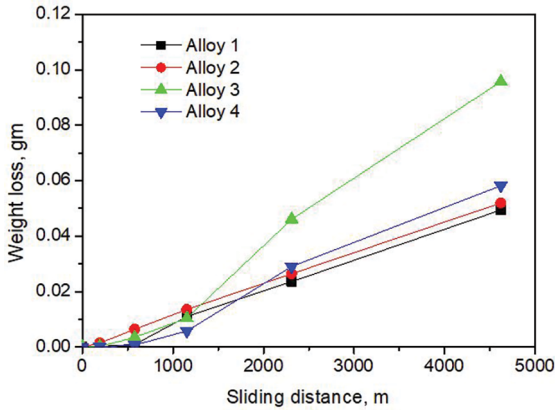


Figure 6. Variation of weight loss with the variation of sliding distance at applied pressure of 1.0MPa (Load = 20N) and sliding velocity of 0.64 ms^{-1}

The influences of sliding distance on wear rate of the alloys at same constant pressure and velocity is shown in Fig. 7. It clearly reveals that as sliding distance increases, wear resistance decreases for all alloys. The increase in wear rate can be attributed to prolonged intimate contact between the two mating surfaces. The presence of the fragmented intermetallics could also weaken the tribolayer and facilitate the initiation and propagation of microcracks probably because of their poor bonding in the tribolayer. These negative effects of β -phase increased with their size and volume fraction and, therefore, Alloy 1 exhibited better wear behaviour than Alloy 2 and Alloy 3 with their higher volume fraction and aspect ratio of intermetallics²⁷. However, Alloy 4 with Cr addition has shown relatively better wear resistance when compared to Alloy 2 and Alloy 3. Cr addition in to the Fe added alloys has resulted in microstructural modifications through changes the beta intermetallics into the modified alpha phases, causes increasing in strength of the alloys thereby reducing the surface damage and increases wear resistance.

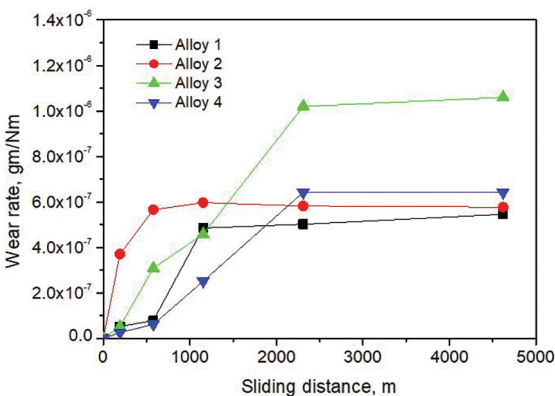


Figure 7. Variation of wear rate (gm/Nm) with the variation of sliding distance at applied pressure of 1.0MPa (Load = 20N) and sliding velocity 0.64 ms^{-1}

The coefficients of friction of all the alloys as a function of the sliding distance is presented in Fig. 8. It can be seen that the coefficient of friction reaches a steady state after showing a sharp increase during the initial sliding distance. The increase of coefficient of friction is due to rough contact surfaces between pin sample and the mild steel disc. Once upon a time they reach an ideal contact, then the result shows almost constant value²⁸. Alloy 2 and Alloy 3 reinforced with hard $\beta\text{-Al}_3\text{FeSi}$ particles, show evidence of higher coefficient of friction than Alloy 1 and Alloy 4. The fine precipitation of Ni intermetallics also responsible for higher friction coefficient in case of Alloy 3²⁹. Alloy 4 shows relatively lower coefficient of friction due to microstructural modification effect by addition of Cr.

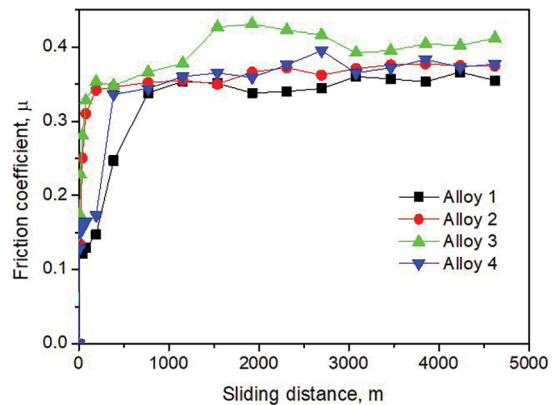


Figure 8. Variation of friction coefficient with the variation of sliding distance at applied pressure of 1.0MPa (Load = 20N) and sliding velocity 0.64 ms^{-1} .

At this time the load also plays a important function on the coefficient of friction. When the load increases slowly, hence the coefficient of friction decreases (Fig. 9). That is the load is indirectly proportional to the co-efficient of friction. This evidently point out that at high loading conditions, the change of phase takes place due to increase in temperature and the material becomes ductile. In case of Ni added Alloy 3 does not show any decreases of coefficient of friction because Ni improve hardness and strength at elevated temperatures and reduce the coefficient of expansion³⁰.

3.3. Optical microscopic observation

The worn surfaces for all the alloys at different sliding distances are presented in Fig. 10. Polished hyper-eutectic Al-Si automotive alloys before wear test consist of an Al-rich dendritic matrix, $\alpha\text{-Al}$ phase and a eutectic mixture in the interdendritic region formed by silicon particles. They are coarse and scattered in plate-like morphology into the matrix³¹. Fe added alloys content mixture of different Fe-rich intermetallics into the alloys. In these type of images dark and lighter two tones are come into view. Precipitates of Al(Mn, Fe, Cu) appear in the dark tone and Al(Si, Mg) appear in a

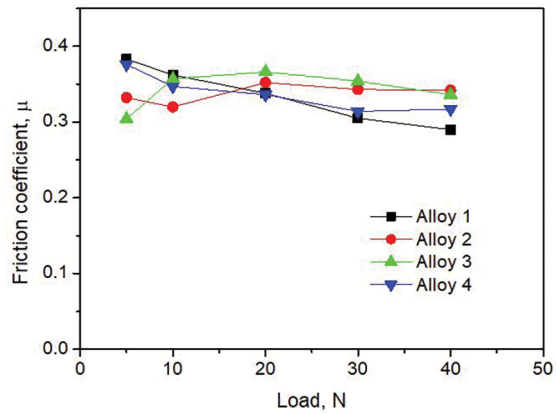


Figure 9. Variation of friction coefficient with applied load at sliding velocity of 0.64 ms^{-1} .

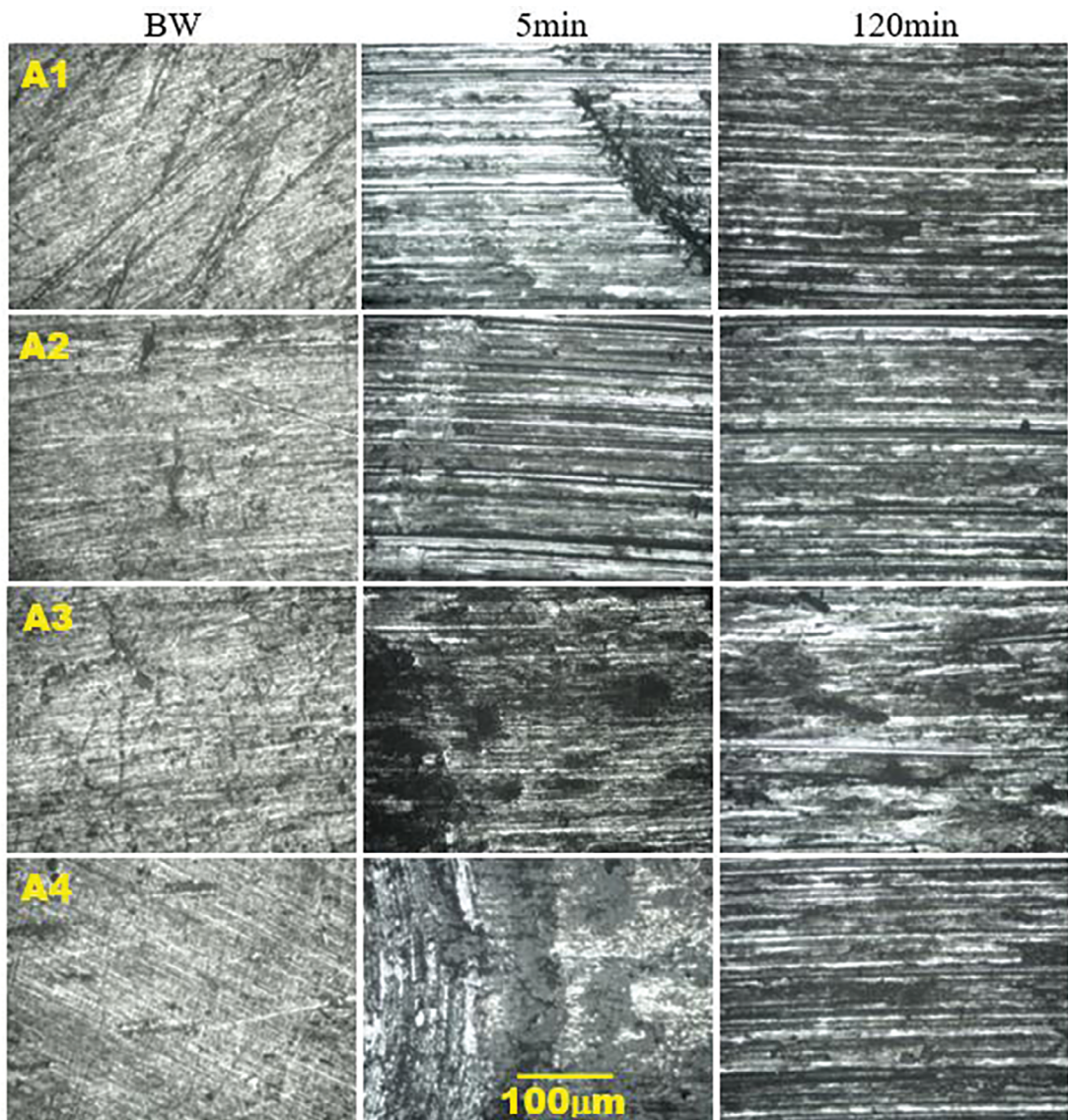


Figure 10. Optical micrograph of worn surfaces of the hyper-eutectic Al-Si automotive base Alloy 1, Fe added Alloy 2, Fe and Ni added Alloy 3 and Fe, Ni and Cr added Alloy 4 at different sliding distances at applied pressure of 1.0 MPa (Load = 20 N) and sliding velocity of 0.64 ms^{-1}

lighter tone respectively. It can be observed that as the sliding distance increase the wear marks becomes more visible and deep for all the alloys. At low sliding distances, the wear marks in the worn surfaces of all the alloys are almost similar in nature whereas at higher sliding distance the wear marks in the worn surfaces are more deep and intense than their higher material loss and corresponding high wear rate. It is due to the creation of $\beta\text{-Al}_5\text{FeSi}$ phase as discussed before. As brittle material has greater wear rate compared to ductile material so surface damage in Alloy 2 and Alloy 3 is higher. Maximum damage on the surface is seen in Alloy 3 as it is the most brittle material here because of the addition of Ni which seems to convert the $\beta\text{-Fe}$ into needle like shape. Alloy 4 is ductile in nature here because of the conversion of harmful $\beta\text{-Fe}$ phase to $\alpha\text{-Fe}$ dendrite.

3.4. Scanning Electron Microscopy

The SEM micrographs of the hyper-eutectic Al-Si automotive Alloy 1, Fe added Alloy 2, Fe and Ni added Alloy 3 and Fe, Ni, and Cr added Alloy 4 are shown in Fig. 11. The microstructures mainly create of primary phase $\alpha\text{-Al}$ dendrites, eutectic Si and an amount of intermetallic phases into the matrix. The presence of Fe, Ni, Cr, Cu and Mg, in the alloy leads to formation of various intermetallic compounds in the microstructure of the alloys. The morphologies of eutectic Si particles are in a form of platelets and acicular. Some void and cavities can be observed in the microstructure of the cast alloys³². In Fig 11b, the microstructure of Fe added Alloy 2 consists of higher amount of $\beta\text{-Al}_5\text{FeSi}$ phase owing the excessive Fe in to the alloy compare to the Alloy 1 (Fig. 11a).

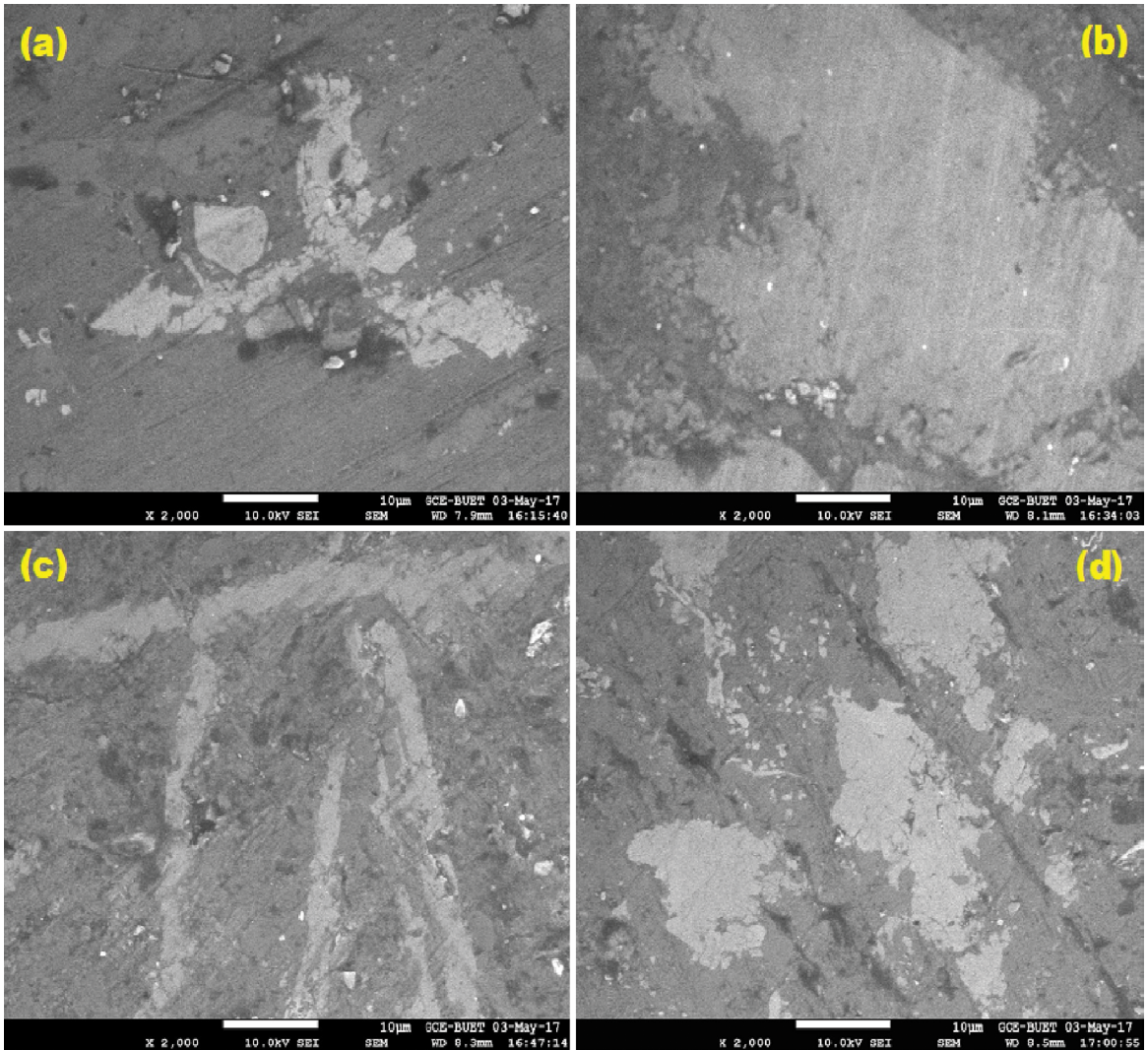


Figure 11. SEM images of the a) hyper-eutectic Al-Si automotive base Alloy 1, b) Fe added Alloy 2, c) Fe and Ni added Alloy 3 and d) Fe, Ni and Cr added Alloy 4.

Alloy 3 contains significant amount of Ni so two types of Al_3Ni phase are the plate-like and needlelike morphologies (Fig. 11c). Fig. 11d shows the SEM micrographs of Cr added Alloy 4 which consists of modified structure with lack of plate-like and needlelike morphologies.

SEM microphotographs of hypereutectic Al-Si automotive base Alloy 1, Fe added Alloy 2, Fe and Ni added Alloy 3 and Fe, Ni and Cr added Alloy 4 after wear test are presented in Fig. 12. The long parallel grooves along the sliding direction, which are caused by the abrasion of entrapped particles, are clearly visible on the worn surfaces of the alloys. Fig. 12a obviously recommend abrasive wear in Alloy 1 revealing grooves due to abrading action by the hard particles which got entrapped. SEM microphotograph exposed small cracks with grooves and dislodging of material clearly indicating combination of abrasive and delaminative wear. The higher

volume fraction of coarser intermetallics in Alloy 2 resulted in a worn surface with subsurface cracks and large facets (Fig. 12b). It seems that the presence of β -particles could facilitate the initiation and the propagation of microcracks in the subsurface regions. These microcracks further could simply propagate through weak interfacial regions of β -platelets and reach to the surface. The presence of large facets of β -platelets in the worn surface confirmed the negative role of β -platelets in the high wear of the Fe rich alloys. Alloy 3 shows the similar fracture surface because addition of Ni does not modify the microstructure of the alloy (Fig. 12c). However, Cr added Alloy 4 has resulted in improved wear resistance, which can be seen through mild abrasive grooves and smooth abrasive grooves filled with oxides (Fig. 12d). It takes place because of the creation of α -Fe dendrite which is relatively ductile in nature³³.

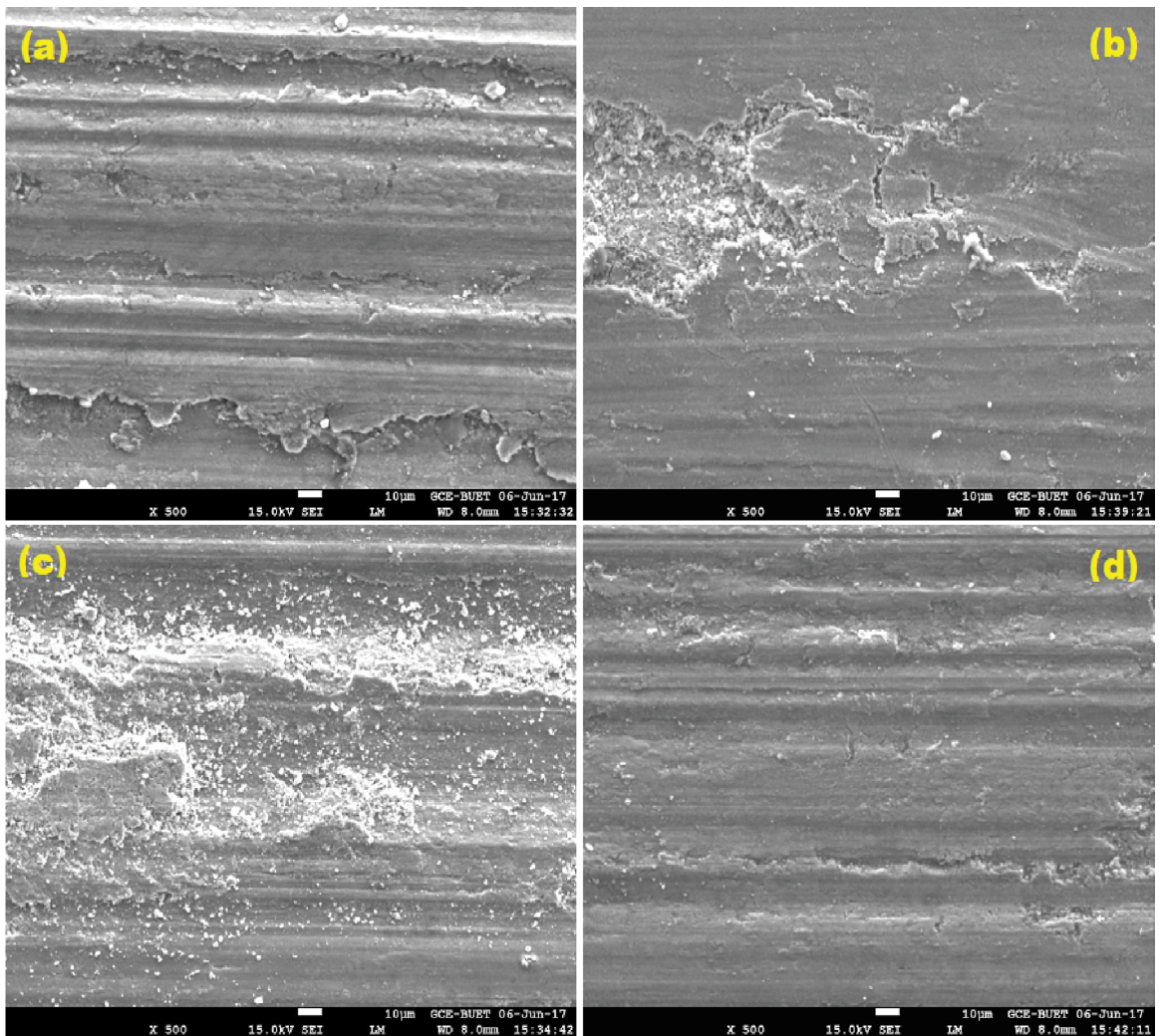


Figure 12. SEM images of the worn surfaces of the a) hyper-eutectic Al-Si automotive base Alloy 1, b) Fe added Alloy 2, c) Fe and Ni added Alloy 3 and d) Fe, Ni and Cr added Alloy 4 after wear for 4600m at applied pressure of 1.0MPa (Load = 20N) and sliding velocity of 0.64 ms^{-1} .

4. Conclusion

Addition of Fe improves the hardness of the hypereutectic Al-Si automotive alloys due to formation of hard β -Al₃FeSi phase. Ni extends the hardness due to precipitation of Ni intermetallic into the aluminium matrix. The Fe bearing intermetallics ensue as stress raisers and points of weakness that reduce the tensile strength and ductility of the alloy. The addition of Cr change in their effectiveness to modify the harmful harder phase to α -Al(Fe, Cr)Si.

The formation of the higher crack sensitive nature of large β -Al₃FeSi needles and primary Fe rich intermetallics which increases the microcracking tendency and decreased the wear resistance of hypereutectic Al-Si automotive alloy. Ni addition more weakens the wear resistance of the alloy. Further addition of Cr has resulted in microstructural changes, recovers strength which is responsible for control of wear and friction.

SEM microphotograph of Fe added alloys exposed subsurface cracks and large facets. However, addition of Cr has resulted in improved wear resistance, which can be seen through mild abrasive grooves and smooth abrasive grooves filled with oxides because of the creation of α -Fe dendrite which is relatively ductile in nature.

5. Acknowledgements

This work is supported by the Department of Mechanical Engineering of Bangladesh University of Engineering and Technology. Thanks to Department of Glass and Ceramics Engineering for providing the laboratory facilities.

6. References

1. Timmermans G, Froyen L. Fretting wear behaviour of hypereutectic P/M Al-Si in oil environment. *Wear*. 1999;230(2):105-117.
2. Kaiser MS, Qadir MR, Dutta S. Electrochemical corrosion performance of commercially used aluminium engine block and piston in 0.1M NaCl. *Journal of Mechanical Engineering*. 2015;45(1):48-52.
3. Subramanain C. Effect of sliding speed on unlubricated wear behaviour of Al-12.3wt.%Si alloy. *Wear*. 1991;151(1):97-110.
4. Kaiser MS, Basher MR, Kurny ASW. Effect of Scandium on Microstructure and Mechanical Properties of Cast Al-Si-Mg Alloy. *Journal of Materials Engineering and Performance*. 2012;21(7):1504-1508.
5. Dwivedi DK. Sliding temperature and wear behaviour of cast Al-Si base alloy. *Materials Science and Technology*. 2003;19(8):1091-1096.
6. Hekmat-Ardakan A, Liu X, Ajersch F, Chen XG. Wear behavior of hypereutectic Al-Si-Cu-Mg casting alloys with Variable Mg contents. *Wear*. 2010;269(9-10):684-692.
7. Yoon H, Sheiretov T, Cusano C. Scuffing behaviour of 390 aluminum against steel under starved lubrication conditions. *Wear*. 2000;237(2):163-175.
8. Clarke J, Sarkar AD. Wear characteristics of as-cast binary aluminium-silicon alloys. *Wear*. 1979;54(1):7-16.
9. Kapranos P, Kirkwood DH, Atkinson HV, Rheinlander JT, Bentzen JJ, Toft PT, et al. Thixoforming of an automotive part in A390 hypereutectic Al-Si alloy. *Journal of Materials Processing Technology*. 2003;135(2-3):271-277.
10. Qin QD, Zhao YG, Zhou W. Dry sliding wear behaviour of Mg₂Si/Al composites against automobile friction material. *Wear*. 2008;264(7-8):654-661.
11. Midson S, Keist J, Svare J. Semi-solid metal processing of aluminum alloy A390. In: *SAE 2002 World Congress & Exhibition*; 2002 Mar 11-15; Detroit, MI, USA. 2002-01-394.
12. Hurtalová L, Tillová E, Chalupová M. Influence of intermetallic phase's on the fracture surfaces in secondary aluminum cast alloy. *Acta Metallurgica Slovaca - Conference*. 2013;3:65-74.
13. Paray F, Gruzleski JE. Microstructure-mechanical property relationships in a 356 alloy. Part I: Microstructure. *Cast Metals*. 1994;7(1):29-40.
14. Murali S, Raman KS, Murthy KSS. Effect of Trace Additions (Be, Cr, Mn and Co) on the Mechanical Properties and Fracture Toughness of Fe-containing Al-7Si-0.3Mg alloy. *Cast Metals*. 1994;6(4):189-198.
15. Petřík J. The application of Ni for improvement of Al-Si-Fe alloys. *Materials Engineering*. 2009;16(4):29-32.
16. Apasi A, Madakson PB, Yawas DS, Aigbodion VS. Wear Behaviour of Al-Si-Fe Alloy/Coconut Shell Ash Particulate Composites. *Tribology in Industry*. 2012;34(1):36-43.
17. Mohan S, Prakash V, Pathak JP. Wear characteristics of HSLA-steel. *Wear*. 2002;252(1-2):16-25.
18. Lin C, Wu S, Lu S, Zeng J, An P. Dry sliding wear behavior of rheocast hypereutectic Al-Si alloys with different Fe contents. *Transactions of Nonferrous Metals Society of China*. 2016;26(3):665-675.
19. Taghiabadi R, Ghasemi HM, Shabestari SG. Effect of iron-rich intermetallics on the sliding wear behavior of Al-Si alloys. *Materials Science and Engineering: A*. 2008;490(1-2):162-170.
20. Zheng Y, Luo B, Bai Z, Wang J, Yin Y. Study of the Precipitation Hardening Behaviour and Intergranular Corrosion of Al-Mg-Si Alloys with Differing Si Contents. *Metals*. 2017;7(387):1-12.
21. Kaiser MS. Solution Treatment Effect on Tensile, Impact and Fracture Behaviour of Trace Zr Added Al-12Si-1Mg-1Cu Piston Alloy. *Journal of the Institution of Engineers (India): Series D*. 2018;99(1):109-114.
22. Geetanjali SG, Veena B, Shivakumar S. Microstructure and Wear Behavior of as Cast Al-25Mg2Si-2Cu-2Ni alloy. *International Journal of Engineering Research*. 2015;4(9):470-474.
23. Ji S, Yang W, Gao F, Watson D, Fan Z. Effect of iron on the microstructure and mechanical property of Al-Mg-Si-Mn and Al-Mg-Si diecast alloys. *Materials Science and Engineering: A*. 2013;564:130-139.

24. Shabestari SG. The effect of iron and manganese on the formation of intermetallic compounds in aluminum-silicon alloys. *Materials Science and Engineering: A*. 2004;383(2):289-298.
25. Mbuya TO, Odera BO, Ng'ang'a SP. Influence of iron on castability and properties of aluminium silicon alloys: Literature review. *International Journal of Cast Metals Research*. 2003;16(5):451-465.
26. Yang Y, Zhong SY, Chen Z, Wang M, Ma N, Wang H. Effect of Cr content and heat-treatment on the high temperature strength of eutectic Al-Si alloys. *Journal of Alloys and Compounds*. 2015;647:63-69.
27. Taghiabadi R, Ghasemi HM. Dry sliding wear behaviour of hypoeutectic Al-Si alloys containing excess iron. *Materials Science and Technology*. 2009;25(8):1017-1022.
28. Ilangovan S. Effect of solidification time on mechanical properties and wear behavior of sand cast aluminium alloy. *International Journal of Research in Engineering and Technology*. 2014;3(2):71-75.
29. Venkateswarlu K, Pathak LC, Ray AK, Das G, Verma PK, Kumar M, et al. Microstructure, tensile strength and wear behaviour of Al-Sc alloy. *Materials Science and Engineering: A*. 2004;383(2):374-380.
30. Jeong CY. Effect of Alloying Elements on High Temperature Mechanical Properties for Piston Alloy. *Materials Transactions*. 2012;53(1):234-239.
31. Kaiser MS. Effects of solution treatment on wear behaviour of Al-12Si-1Mg piston alloy containing trace Zr. *MAYFEB Journal of Materials Science*. 2016;1:27-38.
32. Kaiser MS, Dutta S. Comparison of corrosion behaviour of commercial aluminium engine block and piston in 3.5% NaCl solution. *Advances in Materials Science and Engineering: An International Journal (MSEJ)*. 2014;1(1):9-17.
33. Rana RS, Purohit R, Das S. Reviews on the Influences of Alloying Elements on the Microstructure and Mechanical Properties of Aluminum Alloys and Aluminum Alloy Composites. *International Journal of Scientific and Research Publications*. 2012;2(6):1-7.